

# Automated Plant Light Replenishment Control based Population Intelligence Algorithms in Agricultural Iot Environment

De-Feng Zhou\*

College of Modern Information Engineering  
Hunan Chemical Vocational Technology College  
Zhuzhou 412004, P. R. China  
hnhzyzhou2023@163.com

Sheng-Jie Gan

Information Technology Center  
Hunan Chemical Vocational Technology College  
Zhuzhou 412004, P. R. China  
gansj1983@163.com

Yuan Cui

Department of Basic Courses  
Hunan Chemical Vocational Technology College  
Zhuzhou 412004, P. R. China  
cuiyuan0518@sina.com

Michel X. Virrokni

School of Education  
Grenfell Campus, Memorial University of Newfoundland  
Corner Brook A2H 5G4, Canada  
mxvsvehqnrn1379@gmail.com

\*Corresponding author: De-Feng Zhou  
Received February 21, 2023, revised March 24, 2023, accepted May 20, 2023.

---

**ABSTRACT.** *LED supplemental light arrays have excellent characteristics such as non-polluting, cold light source and low energy consumption, and are therefore widely used in agricultural IoT. However, there is a problem of uneven distribution of LED light replenishment in plant greenhouses. In order to solve the above problems, this work proposes an automated light replenishment control technique based on a population intelligence algorithm. Firstly, the optical structure of the LED array in three-dimensional space is modelled according to Lambert's radiation law. Secondly, a faster-trained extreme learning machine is used to calculate the initial solution, i.e. the position coordinates of blue LEDs and red LEDs, under the same light uniformity condition. The obtained initial solutions are then optimised using an Invasive Weed Optimisation (IWO) algorithm, so that the position parameters of the initial solutions can be further optimised for better light uniformity of the LED complementary array. The experimental results show that the light uniformity of the LED complementary array based on the invasive weed optimisation Extreme Learning Machine (ELM) is improved by 7.1% to 86.7% compared to the common row-by-row LED array. The spectral analysis map obtained after the light supplementation using the ELM-IWO algorithm will be more symmetrical, resulting in a significant improvement of the light conditions and providing an important technical support for the automation of plant culture in the agricultural IoT environment.*

**Keywords:** Internet of things; LED arrays; Light distribution; Invasive weed optimization; Extreme learning machine

---

**1. Introduction.** The light environment is an indispensable physical factor in the growth and development of plants. In the case of greenhouse plants, the indoor light environment has a great influence on the development of the crop. If the light environment in the greenhouse is poor, then the light intensity in some locations may not reach the light compensation point required by the plant [1,2], and the plant may suffer from adverse effects such as reduced photosynthetic efficiency, increased consumption of organic matter, and slowed growth or growth. Therefore, greenhouses need supplemental lighting to promote plant growth [3,4]. If the light source in the greenhouse can be allocated according to the characteristics of plant growth and according to demand, this will ensure the normal growth of the plants and extend their life span.

Light is an important factor for plant growth and development and is therefore a very important parameter throughout the entire growth process. Light has two main effects on plants [5,6,7]: (1) it provides the energy needed for photosynthesis and (2) it regulates plant growth, differentiation and metabolism in the greenhouse. The quality, intensity and duration of light produced by each type of light in a greenhouse varies, and so does its effect on plants. The current mainstream solution is to use LED lights to supplement the plants when there is not enough light to meet the growth needs of the plants. The application of IoT to plant light supplementation systems in greenhouses is a typical example of the combination of agriculture and IoT [8,9]. The technical idea is to establish a scientific, practical and simple system for optimal light intensity data for plants.

The advantages of LED as a fourth generation lighting source include environmental protection, energy savings, minimal heat production, extended service life, as well as high spectral effectiveness and simplicity in management. In order to compensate for the lack of natural light, red and blue LEDs [10,11] have been widely employed as artificial plant light sources. This is because the absorption wavelength of natural light is mostly concentrated in the blue-violet range of 430-450 nm and the red region of 64-660 nm [12].

However, the output light intensity of LEDs is approximately Lambertian distributed, resulting in the non-uniformity of light distribution in the light plane of the LED plant light source array [13,14]. Therefore, in order to solve the problem of uneven distribution of LED light replenishment in plant greenhouses, this work proposes an automated light

replenishment control technique based on a population intelligence algorithm. The main objective of this work is the optimisation of the LED array positions so that the highest light uniformity can be achieved over the entire area, thus ensuring the highest yield in a limited greenhouse area. This work combines Extreme Learning Machines (ELM) [15] and Invasive Weed Optimisation (IWO) [16] to achieve the optimal solution for LED array locations. Firstly, the advantage of random initialisation of the parameters (weights and biases) associated with the ELM single hidden layer feedforward neural network is exploited to improve the time efficiency of the solution. Secondly, the IWO algorithm is used to improve the accuracy of the optimal position solution, providing an important technical support for the automated management of optimal plant culture in the agricultural IoT environment.

**1.1. Related Work.** Compared to traditional light sources, LEDs have significant advantages such as safety, long life, low pollution, low power consumption and small size, and are now widely used in plant lighting, visible light communication and sunlight simulation. They play an important role in modern life. The power of a single LED chip is not sufficient to meet the requirements of an illumination source, so many lighting systems are integrated by multi-chip LED arrays to meet the lighting requirements. Light from unoptimised LED arrays is directly incident on the receiving plane, making it difficult to obtain a uniform lighting effect, so the design of light intensity homogenisation of light from multi-chip LED arrays is of great research value.

In the past few decades, the light distribution of LED light arrays has been a hot topic of research at home and abroad. Su et al. [17] studied the light distribution of LED arrays with different structures by the analytical method theory and found out the LED spacing that could obtain the optimal light uniformity. In order to overcome the complexity of the analytical method, Moreno [18] proposed a method for optimising the design of LED arrays based on a simulated annealing algorithm, and verified the effectiveness of the method by optimising the structural parameters of three different LED arrays. However, the above research mainly focuses on the optimised design of LED light arrays, where there is a better illumination region in the central position of the light plane of the LED light array. However, the uneven illumination can cause differences in the growth of the same batch of plants, thus affecting the cultivation of plants and the study of their light regulation mechanism. Therefore, it is important to realise the problem of finding the optimum light distribution for plant cultivation under LED light arrays to promote the growth of plants and to explore the study of plant light regulation mechanism.

Traditional optimization methods based on geometric and algebraic algorithms are no longer applicable to most current high redundancy systems, so researchers are now mainly using neural networks or intelligent optimization algorithms to solve this type of problems. For example, Gao [19] proposed a back-propagation (BP) neural network-based inverse kinematic solution. Li et al. [20] proposed an adaptive neural network-based all-state observer for solving inverse kinematic models, with the innovation that the adaptive neural network is used to approximate the dead zone function and unknown model of the robot with a smaller error in the initial position of the end-effector. Similar to the above principles based on artificial neural networks, Bendaoud et al. [21] propose an intelligent algorithm that mixes simulated annealing algorithms with genetic algorithms to further improve the accuracy of the optimization search. In Wang et al. [22], a Particle Swarm Optimisation (PSO) algorithm is used to optimise the weight parameters of the neural network in order to improve the performance of the problem solving.

A comparison of the above methods reveals that existing problem finding based on neural networks and intelligent optimization algorithms still have certain disadvantages:

(1) Most of the methods using BP neural networks suffer from the problems of convergence speed and low efficiency of algorithm execution.

(2) Intelligent optimisation using the PSO algorithm or the GA algorithm is more sensitive to the initial centre leading to a tendency to fall into local minima and inaccurate global optimum solutions. This is prominent in the case of uniform light distribution problems with a large number of local optima, resulting in less than ideal accuracy.

**1.2. Motivation and contribution.** Compared with traditional artificial neural networks, ELM has a very high training speed, which helps to improve the execution efficiency when finding the optimum for the uniform light distribution problem. Meanwhile, the Invasive Weed Optimization (IWO) algorithm [23,24] has been proposed and extended by some researchers. The robustness and adaptability of the IWO algorithm are more prominent due to the simulation of weed biology growth patterns. Compared with algorithms such as PSO and GA, the IWO algorithm has better solving ability when dealing with multi-peaked function problems [25].

Therefore, in order to solve the problem of uniform light distribution with more local optima, an automated light supplementation control technique based on invasive weed optimization is proposed in this paper, with the following innovations:

(1) Take advantage of the random initialisation of the ELM input layer weights and hidden layer bias to ensure real-time optimisation of the uniform light distribution search.

(2) Take advantage of the IWO algorithm's better solving ability in dealing with multi-peaked function problems, and take into account both global and local searches to ensure the accuracy of the light uniform distribution search.

## 2. Light distribution structure model.

**2.1. Light distribution of individual LEDs.** The light intensity of a single LED approximates the Lambertian distribution [27].

$$I(\theta) = I_0 \cos^m \theta \quad (1)$$

where  $I(\theta)$  is the light intensity in the direction of the viewing angle  $\theta$  and  $I_0$  is the light intensity in the direction of the LED axis (viewing angle 0).

$$m = \frac{-\ln 2}{\ln(\cos \theta_{1/2})} \quad (2)$$

where  $\theta_{1/2}$  is the angle of view at a light intensity of  $I_0/2$ , called the half-angle.

The illumination produced by an LED located at point  $A(x_0, y_0, 0)$  on the plane of the light source at a distance  $z$  from point  $B(x, y, z)$  on the plane of the light source is shown below:

$$E(x, y, z) = \frac{z^n I_0}{[(x - x_0)^2 + (y - y_0)^2 + z^2]^{\frac{m+2}{2}}} \quad (3)$$

Thus the illumination produced by the LED chip array in three dimensions at the point  $B(x, y, z)$  in the receiving plane is shown below:

$$E(x, y, z) = \sum_{i=1}^N \frac{(z - Z_i)^{m+1} I_0}{[(x - X)^2 + (y - Y)^2 + z^2]^{(m+3)/2}} \quad (4)$$

Approximating the receiving plane  $T$  into  $N$  points, then the average light intensity on the receiving plane  $T$  is shown as follows:

$$\bar{E} = \frac{1}{N} \sum_{i=1}^n E_i \quad (5)$$

The light uniformity of the LED array can be measured by the standard deviation  $\sigma$  of the light intensity on the receiving plane  $T$ . The smaller the  $\sigma$  the smaller the illumination dispersion at each point, i.e. the more uniform the light on the receiving plane. The formula for calculating this  $\sigma$  is as follows:

$$\sigma = \sqrt{\frac{\sum_{i=1}^N (E - E_i)}{N}} \quad (6)$$

**2.2. LED array light distribution.** This work takes a plant light source with a combined red and blue LED distribution as the research object. According to the superposition principle, the red and blue light intensity of the LED plant light source at the point  $B(x, y, z)$  in the light plane is the superposition of the light intensity of all red LEDs and blue LEDs at the point B, respectively [28].

$$E_1(x, y, z) = \sum_i E(x, y, z), i \in \{red, blue\} \quad (7)$$

**2.3. Light uniformity model.** The uniformity of illumination is usually expressed as the quotient of the minimum illumination and the average illumination, with a value between  $[0,1]$ , the larger the value the better the uniformity of illumination. The uniformity of red and blue light on the light plane region  $D$  is expressed as follows:

$$u_1 = \frac{\min\langle E_i(x, y, z) | (x, y) \in D \rangle}{\overline{E}_i} \quad (8)$$

where  $\overline{E}_i$  is the mean light intensity of light over area  $D$ .

$$\overline{E}_i = \frac{1}{S_D} \int E_i(x, y, z) \quad (9)$$

where  $D$  is an area on the light plane and  $S_D$  is the area of light in area  $D$ .

To facilitate numerical calculations, by discretizing the region  $D$  into  $n$  small uniform regions and treating each region as a point, the mean light intensity can be transformed into an expression applicable to the discrete data.

$$\overline{E}_i = \frac{1}{n} \sum_n E_i(x, y, z) \quad (10)$$

The structural model of the light distribution is shown in Figure 1.

### 3. Automated fill light control based on ELM-IWO algorithm.

**3.1. Definition of illuminance uniformity.** In conventional lighting, illuminance in photometry is commonly used to evaluate the light output and lighting effect of a light source, but as photometric parameters are used to represent the response of the human eye to light, their values are influenced by the visual function of the human eye, and the photosynthetic sensitivity curve of plants is somewhat different from the visual function of the human eye, the photometric system is not applicable to the field of plant lighting.

Luminous flux is commonly used in current plant lighting research to assess the effect of light on plants.

$$\Phi = \int_{380}^{780} \nu(\lambda) d\lambda \quad (11)$$

where  $\nu(\lambda)$  indicates the number of moles of photosynthetic photons passing through a unit area per unit time.

$$\Phi_{e,\lambda} = \nu(\lambda) n_A hc / \lambda \quad (12)$$

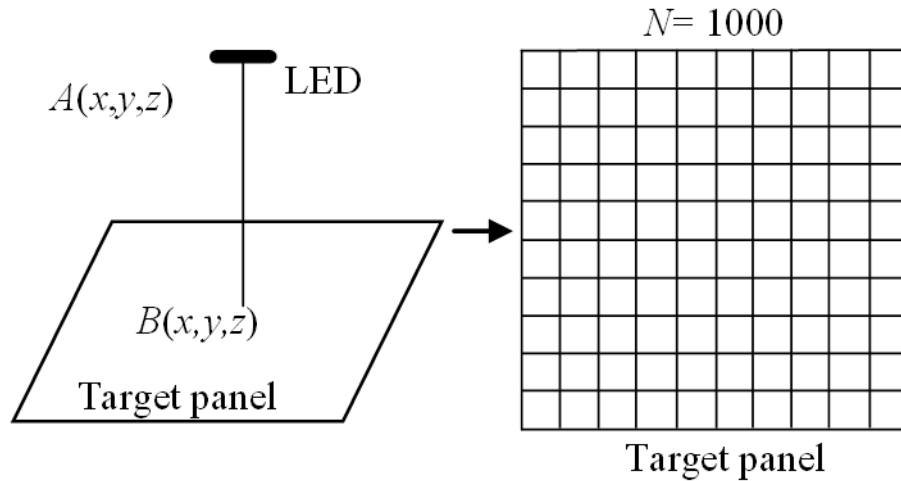


Figure 1. Structural model of light distribution

where  $\Phi_{e,\lambda}$  is the irradiance flux of a beam at a single wavelength  $\lambda$ ,  $n_A$  is Avogadro’s constant and  $hc$  is Planck’s constant.

$$\phi = \int_{380}^{780} \frac{\Phi_{e,\lambda}\lambda}{n_A hc} d\lambda \tag{13}$$

In the visible range the expression for  $D(\lambda)$  can be obtained as follows:

$$D(\lambda) = \int_{380}^{780} \frac{E_{c,\lambda}\lambda}{n_\lambda hc} d\lambda \tag{14}$$

From irradiance and photometric theory, the relationship between optical and radiometric quantities in the visible range is shown as follows:

$$\Phi_v = \int_{380}^{780} K_m \varphi_{e,\lambda} \nu(\lambda) d\lambda \tag{15}$$

Further differential discretization summation is used to normalise the spectral distribution and the light uniformity of  $D(\lambda)$  in the target plane is denoted as  $\mu$ .

$$\mu = \frac{\sum_{x=1}^x \sum_{y=1}^Y \sum_{n=1}^N D(\lambda)/(XYN)}{D(\lambda)_{\max}} \tag{16}$$

Since the spectral range of the red and blue LEDs used in this work can be measured by instruments, the relationship coefficient  $K$  between the illuminance and  $D(\lambda)$  can be accurately calculated, where  $K$  is noted as a constant, so that the light uniformity  $\mu$  is calculated as follows:

$$\mu = \frac{\sum_{x=1}^x \sum_{y=1}^Y \sum_{n=1}^N D(\lambda)/(XYN)}{D(\lambda)_{\max}} = \frac{\frac{1}{K} \sum_{x=1}^x \sum_{j=1}^Y \sum_{n=1}^N E_v/(XYN)}{\frac{1}{K} E_v} \tag{17}$$

**3.2. Construction of ELM.** The traditional method using BP neural network has the problems of slow convergence and low efficiency of algorithm execution because it uses gradient descent to adjust the weights and bias of the neural network, and the extreme learning machine ELM uses a single hidden layer feed-forward architecture, so the learning time is short, and its network structure is shown in Figure 2. The output function of the

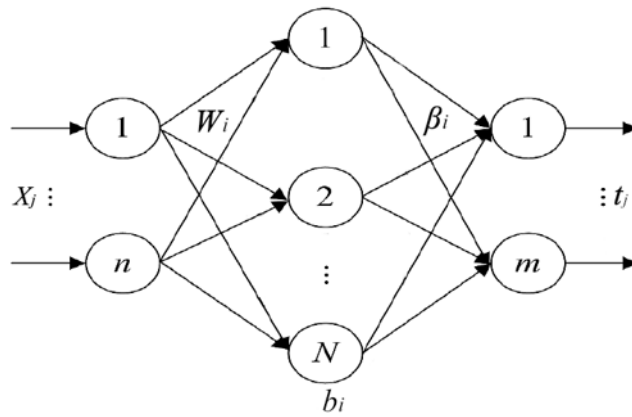


Figure 2. Extreme Learning Machine Network Structure

ELM [29] is shown below:

$$\sum_{i=1}^L \beta_i h(\mathbf{W}_i \bullet \mathbf{X}_j + b_i) = \mathbf{t}_j, \quad (j = 1, 2, \dots, n) \tag{18}$$

where  $b_i$  is the bias of the  $i$ -th hidden node,  $\mathbf{t}_j$  is the output vector,  $\mathbf{X}_j$  is the input vector,  $\mathbf{W}_i$  is the input weight vector,  $\beta_j$  is the output weight vector, and  $h(\cdot)$  is the activation function.

The input weight vectors and biases are generated randomly. The training error is minimised as follow:

$$\|\mathbf{H}\hat{\beta} - \mathbf{T}\| = \min_{\beta} \|\mathbf{H}\beta - \mathbf{T}\|, \beta = \begin{bmatrix} \beta_1^T \\ \beta_2^T \\ \vdots \\ \beta_L^T \end{bmatrix}_{L \times m}, \mathbf{T} = \begin{bmatrix} \mathbf{t}_1^T \\ \mathbf{t}_2^T \\ \vdots \\ \mathbf{t}_N^T \end{bmatrix}_{N \times m} \tag{19}$$

where  $\beta$  represents the output weight matrix and  $\mathbf{T}$  represents the end-effector pose matrix.

Using the least squares method to solve for Equation (19), the output matrix is obtained as

$$\hat{\beta} = \mathbf{H}^\dagger \mathbf{T} \tag{20}$$

where  $\mathbf{H}^\dagger$  denotes the generalised inverse matrix.

$$\mathbf{H}\beta = \mathbf{T} \tag{21}$$

$\mathbf{H}$  and  $\beta$  are multiplied as shown as follow:

$$H(w_1, \dots, w_N, b_1, \dots, b_N, x_1, \dots, x_N) = \begin{bmatrix} g(w_1 \cdot x_1 + b_1) & \dots & g(w_N \cdot x_1 + b_N) \\ \vdots & \dots & \vdots \\ g(w_1 \cdot x_N + b_1) & \dots & g(w_N \cdot x_N + b_N) \end{bmatrix}_{N \times N} \tag{22}$$

We need to find the right values for  $\hat{w}_i$ ,  $\hat{b}_i$  and  $\hat{\beta}_i$  to obtain a stable model of the network structure.

$$\left\| H(\hat{w}_1, \dots, \hat{w}_N, \hat{b}_1, \dots, \hat{b}_N) \beta^\wedge - \mathbf{T} \right\| = \min_{w_i, b_i, \beta} \left\| H(w_1, \dots, w_N, b_1, \dots, b_N) \beta - \mathbf{T} \right\| \tag{23}$$

$$E = \sum_{j=1}^N \left( \sum_{i=1}^{\tilde{N}} (\beta_i g(w_i \cdot x_j = b_i) - t_j)^2 \right) \quad (24)$$

To solve for the minimal values of  $\|H\beta - T\|$ , the values of  $(w_i, \beta_i)$  in the neural network structure are represented as a matrix  $W$  and solved for using the gradient descent method.

$$W_k = W_{k-1} - \eta \frac{\partial E(W)}{\partial W} \quad (25)$$

where  $\eta$  denotes the learning step [30].

The structural model of the illuminance distribution is solved by ELM to obtain an initial solution for the optimisation of the LED array position.

**3.3. Principles of the IWO algorithm.** 3.3. Principles of the IWO algorithm. Plants known biologically as weeds generally exhibit tenacity, outstanding reproductive capacity and short growth cycles, and are more resistant and environmentally adaptable than crops. in 1962, Mac Arthur proposed the theory of population reproduction to investigate the reproduction and competitive elimination strategies of populations.

IWO is a swarm intelligence optimisation algorithm that simulates the growth and reproduction strategy of weed occupancy and is used to solve constrained problems with the following characteristics: (1) reproduction rules based on fitness values; (2) seed dispersal following a normal distribution; and 3) a gentle competitive exclusion mechanism.

The IWO algorithm achieves the solution of a typical problem optimisation by means of 4 main operations.

(1) Population initialization operation. A random principle is used to scatter weeds, the first generation seed population, over the solution space, where the seed locations represent the required solutions to the constraint problem function. In addition, a first evaluation of the fitness values of all seed locations is required.

(2) Weed propagation operation. The propagation operation is performed after sorting the weed seed fitness values (from largest to smallest), as shown in Figure 3

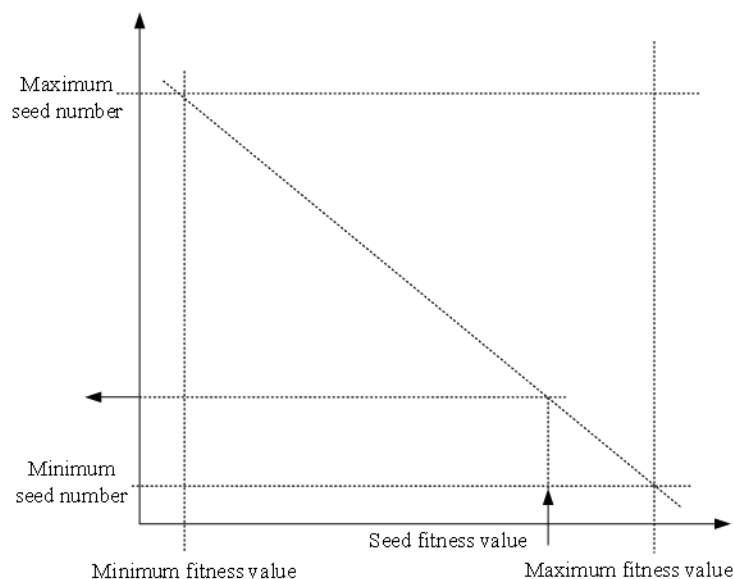


Figure 3. Schematic representation of the principle of weed reproduction

Weeds follow the reproduction protocols shown as follow:

$$S_a(h+1) = \left\lfloor \frac{f_{\max}(h) - f(q_a(h))}{f_{\max}(h) - f_{\min}(h)} \cdot (S_{\max} - S_{\min}) \right\rfloor + S_{\min}, \forall a = 1, 2, \dots, m(h) \quad (26)$$

where  $q_a(h)$  is the current position of weed  $a$  after the  $h$ -th iteration,  $f_{\max}(h)$  and  $f_{\min}(h)$  are the maximum and minimum fitness of the population after the  $h$ -th iteration, respectively.  $m(h)$  is the number of weeds after the  $h$ -th iteration, and  $f(q_a(h))$  is the fitness of weed  $a$  at the current position. The operator  $\lfloor \cdot \rfloor$  indicates rounding down,  $S_{\max}$  and  $S_{\min}$  are the maximum and minimum number of seeds that the weed can produce, respectively.

(3) Spatial diffusion operation of seeds. As the number of iterations increases, the standard deviation decreases, thus ensuring a gap between the offspring and the parent. The standard deviation is calculated as shown as follow:

$$\sigma_j(h+1) = \frac{(h_{\max} - h - 1)^\psi (\sigma_{\max,j} - \sigma_{\min,j})}{h_{\max}^\psi} + \sigma_{\min,j}, \forall j = 1, 2, \dots, D \quad (27)$$

where  $\psi$  is the non-linear modulation index, which usually takes the value of 2.  $\sigma_{\max,j}$  and  $\sigma_{\min,j}$  are the maximum and minimum standard deviation of the  $j$  dimensional component of the  $D$ -dimensional solution space, respectively.  $h_{\max}$  is the maximum number of iterations.

(4) Competitive culling operation. After the reproduction and dispersal operations described above, the parent population and its progeny are sorted together from largest to smallest according to their fitness value and a new reproduction operation is started, with all other weed individuals discarded.

The above four iterations are repeated until the maximum number of iterations is reached, at which point the position of the most adapted weed in the population is the output of the optimization process.

**3.4. 3D LED array optimisation based on ELM-IWO.** The optimization problem of this work is to find the optimal position of the blue and red complementary light irradiation. The LED array is considered as the set of all weeds, and the location of each LED is considered as the location that can be reached after the weed reproduction and diffusion operation.

In practice, the problem of uneven light for plants has a significant impact on greenhouses. Parts of the same greenhouse are susceptible to the influence of surrounding shade and the movement of the sun at different times, resulting in the entire area of the greenhouse not meeting the expected demand. In order to maximise the yield per area of the greenhouse, we need to ensure that the maximum yield is achieved in a limited area of the greenhouse. By solving the light problem, we can maximise crop yields in a limited area. Therefore, how to maximise the yield per area of greenhouse is an urgent problem to solve. By comparing the currently collected real-time light intensity values with the light intensity values provided by expert empirical data, the ELM-IWO algorithm is used to drive the fill light arrays and to optimise the position of the LED fill lights as much as possible, so that the entire area can be optimally illuminated.

The optimization problem is to find the optimal fitness. The fitness function  $F_{fitness}$  is set as the objective function of the IWO algorithm in the 3D LED array optimization search, thus promoting better and faster growth of greenhouse crops. Weeds continue to multiply and spread through iterations to achieve the optimisation of the objective function. Equation (6) is set as the convergence condition of the function, and the position coordinates of the LED light array can be obtained after the algorithm is optimised.

$$F_{fitness} = \sqrt{(T' - T)^2} = \sqrt{(p'_x - p_x)^2 + (p'_y - p_y)^2 + (p'_z - p_z)^2} \quad (28)$$

$$T' = (p_x, p_y, p_z, o_x, o_y, o_z, a_x, a_y, a_z, n_x, n_y, n_z) \quad (29)$$

where  $T$  is the initial solution position coordinate calculated by ELM,  $T'$  is the input position coordinate.

#### 4. Experimental results and analysis.

**4.1. Selection of light sources.** Based on the commonly used LED plant light sources, a rectangular structured LED light array was selected for the study.

The plant light array is a rectangular structure of 12 rows and 14 columns of LEDs, with a row and column spacing of 2 cm. 168 LEDs are present on the light source, with a 1:1 ratio of red to blue LEDs, and the red and blue LEDs are staggered along the rows and columns. The distance from the illumination plane to the corresponding light source plane is 20 cm, and a Cartesian coordinate system is established with the centre of the plant light source as the origin.

**4.2. Optimisation results.** The optimization process of the 3D LED array based on the ELM-IWO algorithm is shown in Figure 4. During the iterations, the optimal value of

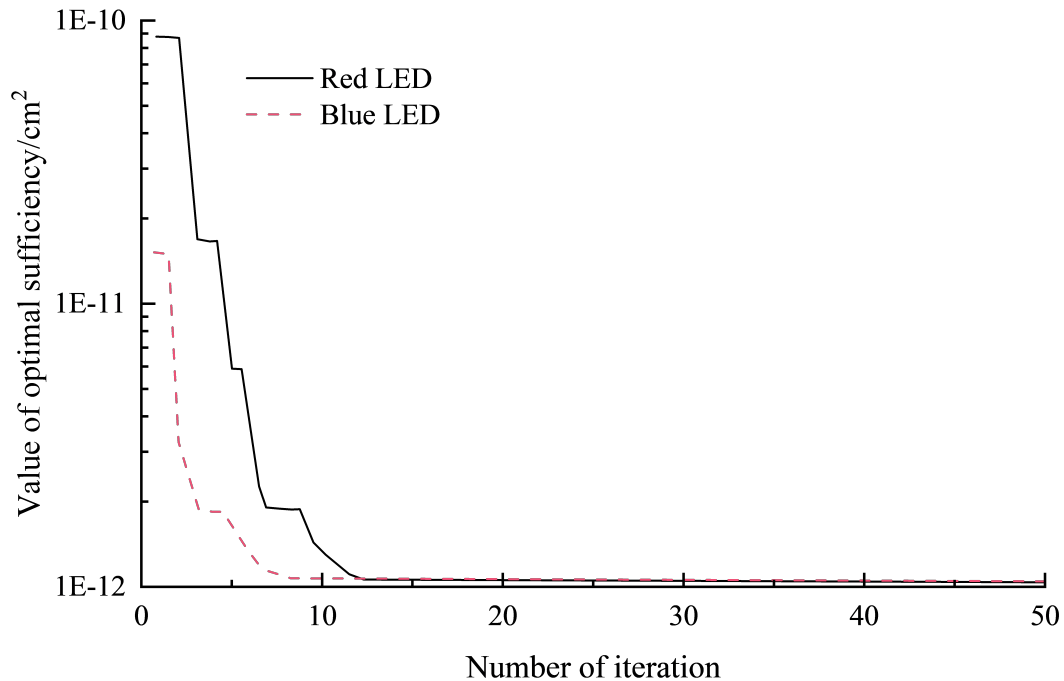


Figure 4. Iterative process of ELM-IWO algorithm

IWO gradually approximates the optimal solution of the uniform illumination distribution problem, and after only about 25 iterations, the optimization process has started to converge to a stable value, indicating the high efficiency of the method. The results of the 3D LED array coordinate parameter search are shown in Table 1.

Table 1. Optimized coordinates of 3D LED array

	1	2	3	4	5	6	7	8	9
$x$	25	0	-25	25	0	-25	25	0	-25
$y$	25	25	25	0	0	0	-25	-25	-25
$z$	0.1321	0.0863	0.0926	0.0539	0.2126	0.0709	0.0934	0.0681	0.0852

**4.3. Selection of reference light intensity measurement points.** In order to compare the current light supplementation situation with the results after applying the ELM-IWO algorithm for light supplementation, a 15 m x 25 m area of the greenhouse was randomly selected for light intensity analysis.

Due to the large size of the greenhouse, measurement points were randomly selected to reflect the current light conditions in the greenhouse as well as the light fill. The 48 measurement points were selected at random, all of which were chosen at random, so that the results are indicative and provide an accurate picture of the greenhouse conditions. The randomly selected light measurement points are shown in Figure 5.

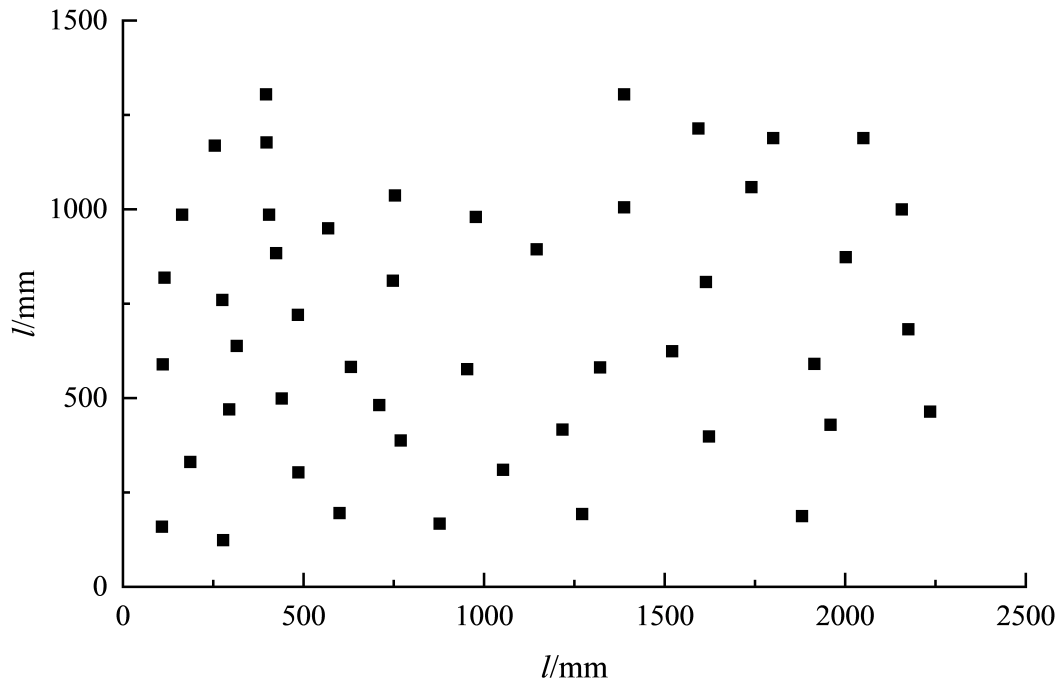


Figure 5. Random light measurement point

**4.4. Comparison of light supplementation performance.** A two-dimensional plot of light intensity analysis for a randomly selected day during the growing process is shown in Figure 6.

It can be seen that the light is stronger in the upper part and weaker in the lower part. This is due to the fact that under normal circumstances, the upper part of the greenhouse would have sunlight coming in, not only from directly above but also from the side, as it is located at the top part of the plot. For the end part, the side light is also available, but due to the siting of this experiment (there is a wall at the end of the greenhouse), the light intensity from the surrounding area is blocked, so the direct light intensity from the outside is weaker there. At the bottom end the light intensity is very weak, which is the reason for the siting problem. However, the difficulties encountered in these experiments can be overcome in the course of subsequent experiments by means of supplementary lighting.

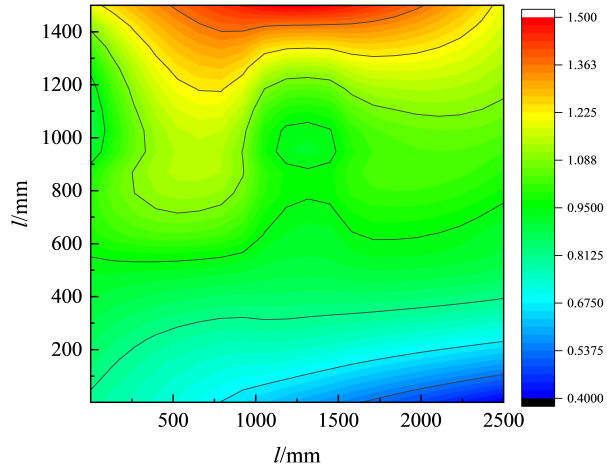


Figure 6. Normal conditions

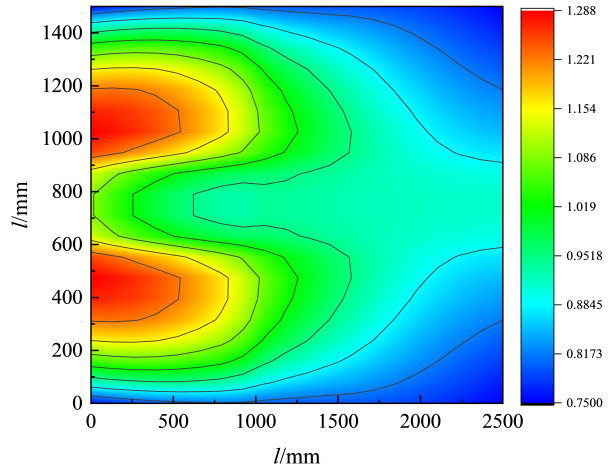


Figure 7. Applied algorithms

The above scenarios are measurements taken under normal light conditions without any measures. A two-dimensional plot of the light intensity distribution of the light supplementation using the ELM-IWO algorithm under normal light conditions is shown in Figure 7. We can clearly see that the spectral analysis plot obtained after the light replenishment using the ELM-IWO algorithm will be more symmetrical and that all parts have basically met the optimum light conditions for the plant for that growth period, which means that the new light conditions have been substantially improved.

The illuminance distribution of the unoptimised and optimised LED arrays are shown in Figure 8 and Figure 9 respectively. It can be seen that the uniformity of illuminance of the unoptimised LED array is 79.60 %, while the uniformity of illuminance of the optimised LED array is improved by 7.1% to 86.7 %, which significantly improves the illumination effect and verifies the effectiveness of the proposed method.

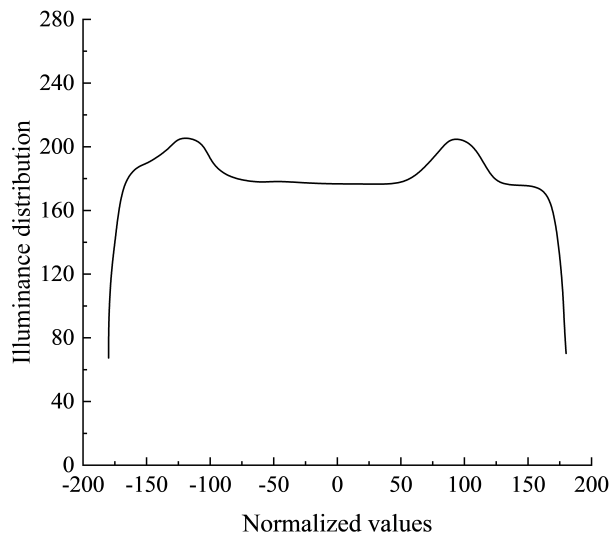


Figure 8. Unoptimised illuminance

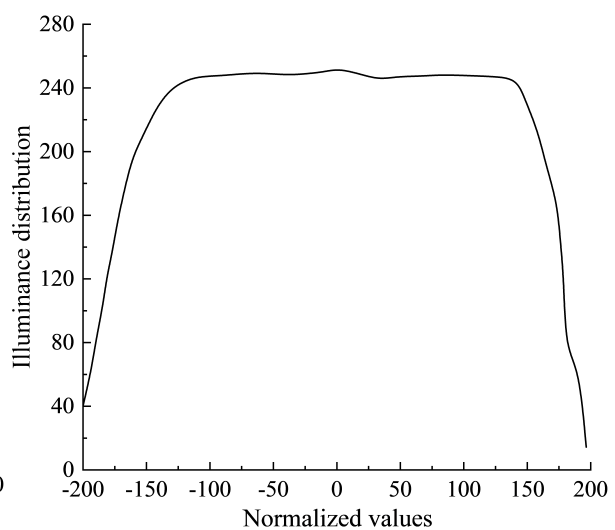


Figure 9. Optimised illuminance

**5. Conclusion.** In order to improve the uniformity of light sources in LED plant lighting arrays, this work presents an automated light supplementation control technique based on a population intelligence algorithm. An Extreme Learning Machine (ELM) and Invasive Weed Optimisation (IWO) are combined to achieve an optimal solution for the LED array position. Firstly, the advantage of random initialisation of the parameters (weights and biases) associated with the ELM single hidden layer feedforward neural network is exploited to improve the time efficiency of the solution. Secondly, the IWO algorithm is used to improve the accuracy of the optimal position solution. Compared to common row-by-row LED arrays, the light uniformity of the invasive weed optimised extreme learning machine based LED fill light array improved by 7.1 % to 86.7 %. The spectral analysis maps obtained after the light supplementation using the ELM-IWO algorithm will be more symmetrical, resulting in a substantial improvement in light conditions. Follow-up studies will attempt to use multi-objective or parallelised intelligent optimisation algorithms to control the light source of the LED plant lighting array in order to achieve greater light uniformity with greater efficiency.

**Funding Statement.** This work supported by the Natural Science Foundation of Hunan Province (No. 2022JJ50090).

## REFERENCES

- [1] C.-M. Chen, Z. Chen, S. Kumari, and M.-C. Lin, "LAP-IoHT: A Lightweight Authentication Protocol for the Internet of Health Things," *Sensors (Basel, Switzerland)*, vol. 22, no. 14, 5401, 2022.
- [2] Y.-Q. Chen, B. Zhou, M. Zhang, and C.-M. Chen, "Using IoT technology for computer-integrated manufacturing systems in the semiconductor industry," *Applied Soft Computing*, vol. 89, 106065, 2020.
- [3] T.-Y. Wu, F. Kong, Q. Meng, S. Kumari, and C.-M. Chen, "Rotating behind security: an enhanced authentication protocol for IoT-enabled devices in distributed cloud computing architecture," *EURASIP Journal on Wireless Communications and Networking*, vol. 2023, no. 1, 36, 2023.
- [4] T.-Y. Wu, H. Li, and S.-C. Chu, "CPPE: An Improved Phasmatodea Population Evolution Algorithm with Chaotic Maps," *Mathematics*, vol. 11, no. 9, 1977, 2023.
- [5] T.-Y. Wu, Q. Meng, Y.-C. Chen, S. Kumari, and C.-M. Chen, "Toward a Secure Smart-Home IoT Access Control Scheme Based on Home Registration Approach," *Mathematics*, vol. 11, no. 9, 2123, 2023.
- [6] T.-Y. Wu, A. Shao, and J.-S. Pan, "CTOA: Toward a Chaotic-Based Tumbleweed Optimization Algorithm," *Mathematics*, vol. 11, no. 10, 2339, 2023.
- [7] Z. Yang, Y. Ding, K. Hao, and X. Cai, "An adaptive immune algorithm for service-oriented agricultural Internet of Things," *Neurocomputing*, vol. 344, pp. 3-12, 2019.
- [8] K. Huang, L. Shu, K. Li, F. Yang, G. Han, X. Wang, and S. Pearson, "Photovoltaic agricultural internet of things towards realizing the next generation of smart farming," *IEEE Access*, vol. 8, pp. 76300-76312, 2020.
- [9] T. Ojha, S. Misra, and N. S. Raghuvanshi, "Internet of things for agricultural applications: The state of the art," *IEEE Internet of Things Journal*, vol. 8, no. 14, pp. 10973-10997, 2021.
- [10] F. Wu, and J. Ma, "Evolution dynamics of agricultural internet of things technology promotion and adoption in China," *Discrete Dynamics in Nature and Society*, vol. 2020, pp. 1-18, 2020.
- [11] Y. Liu, D. Li, B. Du, L. Shu, and G. Han, "Rethinking sustainable sensing in agricultural Internet of Things: From power supply perspective," *IEEE Wireless Communications*, vol. 29, no. 4, pp. 102-109, 2022.
- [12] X. Zou, W. Liu, Z. Huo, S. Wang, Z. Chen, C. Xin, Y. Bai, Z. Liang, Y. Gong, and Y. Qian, "Current Status and Prospects of Research on Sensor Fault Diagnosis of Agricultural Internet of Things," *Sensors*, vol. 23, no. 5, 2528, 2023.
- [13] C. Zhang, and Z. Liu, "Application of big data technology in agricultural Internet of Things," *International journal of distributed sensor networks*, vol. 15, no. 10, 1550147719881610, 2019.
- [14] C. Verdouw, S. Wolfert, and B. Tekinerdogan, "Internet of Things in agriculture," *CABI Reviews*, no. 2016, pp. 1-12, 2016.

- [15] A. Tzounis, N. Katsoulas, T. Bartzanas, and C. Kittas, "Internet of Things in agriculture, recent advances and future challenges," *Biosystems Engineering*, vol. 164, pp. 31-48, 2017.
- [16] X. Zhang, Z. Cao, and W. Dong, "Overview of edge computing in the agricultural internet of things: key technologies, applications, challenges," *IEEE Access*, vol. 8, pp. 141748-141761, 2020.
- [17] Z. Su, D. Xue, and Z. Ji, "Designing LED array for uniform illumination distribution by simulated annealing algorithm," *Optics Express*, vol. 20, no. 106, pp. A843-A855, 2012.
- [18] I. Moreno, "Image-like illumination with LED arrays: design," *Optics Letters*, vol. 37, no. 5, pp. 839-841, 2012.
- [19] R. Gao, "Inverse kinematics solution of Robotics based on neural network algorithms," *Journal of Ambient Intelligence and Humanized Computing*, vol. 11, no. 12, pp. 6199-6209, 2020.
- [20] Y. Li, Y. Liu, and S. Tong, "Observer-based neuro-adaptive optimized control of strict-feedback nonlinear systems with state constraints," *IEEE Transactions on Neural Networks and Learning Systems*, vol. 33, no. 7, pp. 3131-3145, 2021.
- [21] R. Bendaoud, H. Amiry, M. Benhmida, B. Zohal, S. Yadir, S. Bounouar, C. Hajjaj, E. Baghaz, and M. El Aydi, "New method for extracting physical parameters of PV generators combining an implemented genetic algorithm and the simulated annealing algorithm," *Solar Energy*, vol. 194, pp. 239-247, 2019.
- [22] Y. Wang, H. Zhang, and G. Zhang, "cPSO-CNN: An efficient PSO-based algorithm for fine-tuning hyper-parameters of convolutional neural networks," *Swarm and Evolutionary Computation*, vol. 49, pp. 114-123, 2019.
- [23] M. Misaghi, and M. Yaghoobi, "Improved invasive weed optimization algorithm (IWO) based on chaos theory for optimal design of PID controller," *Journal of Computational Design and Engineering*, vol. 6, no. 3, pp. 284-295, 2019.
- [24] L. Huang, P. G. Asteris, M. Koopialipoor, D. J. Armaghani, and M. Tahir, "Invasive weed optimization technique-based ANN to the prediction of rock tensile strength," *Applied Sciences*, vol. 9, no. 24, 5372, 2019.
- [25] W. Wang, G. Tian, G. Yuan, and D. T. Pham, "Energy-time tradeoffs for remanufacturing system scheduling using an invasive weed optimization algorithm," *Journal of Intelligent Manufacturing*, vol. 11, no.4, pp. 1-19, 2021.
- [26] A. Goli, E. B. Tirkolaee, B. Malmir, G.-B. Bian, and A. K. Sangaijah, "A multi-objective invasive weed optimization algorithm for robust aggregate production planning under uncertain seasonal demand," *Computing*, vol. 101, pp. 499-529, 2019.
- [27] H. Inagaki, A. Saito, H. Sugiyama, T. Okabayashi, and S. Fujimoto, "Rapid inactivation of SARS-CoV-2 with deep-UV LED irradiation," *Emerging Microbes & Infections*, vol. 9, no. 1, pp. 1744-1747, 2020.
- [28] K. Zhang, N. Zhu, M. Zhang, L. Wang, and J. Xing, "Opportunities and challenges in perovskite LED commercialization," *Journal of Materials Chemistry C*, vol. 9, no. 11, pp. 3795-3799, 2021.
- [29] J. S. Manoharan, "Study of variants of extreme learning machine (ELM) brands and its performance measure on classification algorithm," *Journal of Soft Computing Paradigm (JSCP)*, vol. 3, no. 2, pp. 83-95, 2021.
- [30] S. Lu, S.-H. Wang, and Y.-D. Zhang, "Detection of abnormal brain in MRI via improved AlexNet and ELM optimized by chaotic bat algorithm," *Neural Computing and Applications*, vol. 33, pp. 10799-10811, 2021.